

Element Quality Metrics for Higher-Order Bernstein–Bézier Elements

Luke Engvall and John A. Evans

Abstract In this note, we review the interpolation theory for curvilinear finite elements originally derived by Ciarlet and Raviart [1]. Specifically, we highlight the sufficient conditions for guaranteeing a sequence of (possibly non-nested) meshes will preserve optimal convergence rates, and we argue that existing curvilinear quality metrics are not sufficient for guaranteeing that these conditions hold. We then present a set of curvilinear element quality metrics which are inspired by these conditions. These quality metrics, along with existing element quality metrics, are sufficient for showing that a series of refined Bernstein–Bézier meshes will preserve optimal convergence rates.

1 Notation

Let us denote a unit reference element in parametric space $\hat{\Omega}$. Then we denote the element in physical space Ω_e , and denote a mapping \mathbf{x}_e that maps points on the parametric element to points on the physical element. We also consider the element $\bar{\Omega}_e$ which is the *purely linear* physical element. That is, $\bar{\Omega}_e$ is defined by an affine mapping $\bar{\mathbf{x}}_e$. These mappings are illustrated in Fig. 1. We note that for simplicial elements, the linear physical element is simply defined as the linear interpolant of the corners of the curvilinear physical element. However, for tensor product elements (i.e. quadrilaterals or hexahedra), the affine element will not necessarily interpolate every corner of the curvilinear element, as seen in Fig. 1. This is due to the fact that the tensor product admits bilinear mappings for quadrilaterals and trilinear mappings for hexahedra.

Luke Engvall
Coreform LLC, 1427 S 550 E, Orem, UT 84097, e-mail: lukeengvall@coreform.tech

John A. Evans
University of Colorado Boulder, 1111 Engineering Drive, Boulder, CO 80309 e-mail:
John.A.Evans@colorado.edu

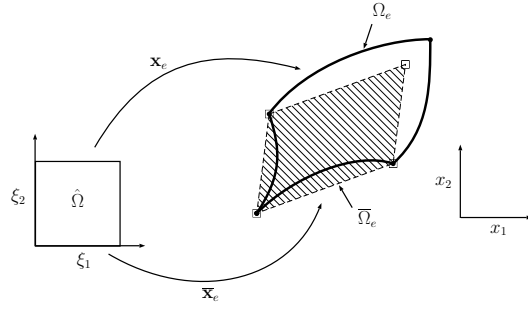


Fig. 1 Isoparametric mappings from a reference element $\hat{\Omega}$ in parametric space to physical space. The element Ω_e (bold line) is defined by the mapping \mathbf{x}_e . The linear element $\bar{\Omega}_e$ (dashed line) is defined by a purely affine mapping $\bar{\mathbf{x}}_e$.

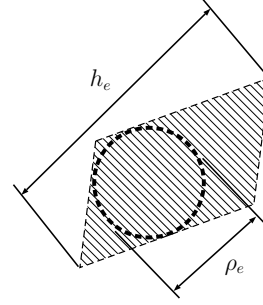


Fig. 2 Element size metrics h_e (element diameter) and ρ_e (incircle diameter) for the linear element $\bar{\Omega}_e$.

In the finite element method, we approximate a domain Ω using a set of finite elements, $\{\Omega_e\}_{e=1}^E$, where each element $\Omega_e \in \mathbb{R}^d$ is an open simply connected set, with simply connected boundary. Together, this collection of elements forms a finite element discretization or mesh, which we denote as:

$$\mathcal{M} = \overline{\bigcup_{e=1}^E \Omega_e}$$

Furthermore, we denote the diameter of an element as h_e and the diameter of the incircle (in \mathbb{R}^2) or insphere (in \mathbb{R}^3) of the element as ρ_e . These two metrics are visualized for a quadrilateral element in Fig. 2. Given these element-wise measures, we can then define the corresponding global mesh measures as:

$$h = \max_{1 \leq e \leq E} h_e$$

$$\rho = \min_{1 \leq e \leq E} \rho_e$$

These mesh measures allow us to introduce the notion of *shape regularity*. For a mesh of linear elements, the mesh shape regularity is given by:

$$\sigma = \frac{h}{\rho}$$

Now, let us consider a set of M increasingly refined *linear* meshes $\{\bar{\mathcal{M}}\}_{i=1}^M$, with corresponding metrics $\{h_i\}_{i=1}^M$ and $\{\rho_i\}_{i=1}^M$ where $h_1 > h_2 > \dots > h_M$. We say that the refinements lead to a *regular family* of elements if we can bound the mesh shape regularity σ_i by some constant σ_0 , viz.:

$$\sigma_i \leq \sigma_0 \quad i = 1, 2, \dots, M$$

2 Literature Review

The interpolation theory for curvilinear finite elements was originally derived by Ciarlet and Raviart [1], and we briefly review the central result of the theory here. Let us denote a sequence of refined curvilinear meshes $\{\mathcal{M}_i\}_{i=1}^M$, and let the following conditions hold for every element in each mesh.

Cond. (2.1) The underlying linear elements $\overline{\Omega}_e$ belong to a regular family.

Cond. (2.2) The mapping \mathbf{x}_e is invertible. That is:

$$\mathbf{x}_e(\boldsymbol{\xi}) = \mathbf{x} \Leftrightarrow \mathbf{x}_e^{-1}(\mathbf{x}) = \boldsymbol{\xi} \quad \forall \boldsymbol{\xi} \in \hat{\Omega}$$

Cond. (2.3) The derivatives of the mapping, $D_{\boldsymbol{\xi}}^{\boldsymbol{\alpha}} \mathbf{x}_e$, are bounded as follows:

$$\begin{aligned} \sup_{\boldsymbol{\xi} \in \hat{\Omega}} \max_{|\boldsymbol{\alpha}|=k} |D_{\boldsymbol{\xi}}^{\boldsymbol{\alpha}} \mathbf{x}_e| &\leq c_k h^k \quad 1 \leq k \leq p+1 \\ \sup_{\mathbf{x} \in \Omega_e} \max_{|\boldsymbol{\alpha}|=1} |D_{\mathbf{x}}^{\boldsymbol{\alpha}} (\mathbf{x}_e^{-1})| &\leq c_0 h^{-1} \end{aligned}$$

Then, for a series of meshes belonging to a regular family, we have the error bound:

$$\|u - u_h\|_{H^m(\Omega)} \leq C \frac{\sup_{\boldsymbol{\xi} \in \hat{\Omega}} |\det \mathbf{x}_e|}{\inf_{\boldsymbol{\xi} \in \hat{\Omega}} |\det \mathbf{x}_e|} h^{p+1-m} \|u\|_{H^{p+1}(\Omega)} \quad (1)$$

wherein C is a constant independent of the mesh size h , and $\|\cdot\|_{H^m(\Omega)}$ denotes the norm:

$$\|f\|_{H^m(\Omega)} = \left(\sum_{j=0}^m |f|_{H^j(\Omega)}^2 \right)^{1/2}$$

and $|\cdot|_{H^j(\Omega)}$ denotes the seminorm:

$$|f|_{H^j(\Omega)} = \left(\int_{\Omega} \sum_{|\boldsymbol{\alpha}|=j} |D^{\boldsymbol{\alpha}} f|^2 d\Omega \right)^{1/2}$$

From this, we see that for a curvilinear mesh to exhibit similar convergence rates to a linear mesh, several criteria must hold. First, as before, the underlying linear elements must be shape-regular (Cond. 2.1). However, we must also ensure that the higher-order mapping is invertible (Cond. 2.2), and that its derivatives are bounded (Cond. 2.3). If the mapping \mathbf{x}_e becomes singular, then $\inf_{\boldsymbol{\xi} \in \hat{\Omega}} |\det \mathbf{x}_e| = 0$, and the error

bounds in Eq. (1) will tend towards infinity.

It is perhaps due to this observation that the overwhelming majority of curvilinear quality metrics are based on some measure of the Jacobian matrix. Of these Jacobian based quality metrics, perhaps the most commonly used curvilinear quality metric

is the *scaled Jacobian* [2], defined as:

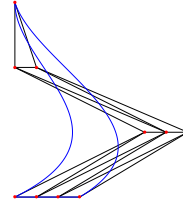
$$J_S = \frac{\inf_{\xi \in \hat{\Omega}} |\det \mathbf{x}_e|}{\sup_{\xi \in \hat{\Omega}} |\det \mathbf{x}_e|} \quad (2)$$

From Eq. (2), it is readily apparent that $0 \leq J_S \leq 1$, with element quality increasing as $J_S \rightarrow 1$. For an affine element, the Jacobian is constant across the element, and the metric is identically unity. For a singular or inverted element, $\inf_{\xi \in \hat{\Omega}} |\det \mathbf{x}_e| = 0$, and the metric is zero.

Besides the scaled Jacobian, there have been other proposed higher order quality metrics all based on some measure of the Jacobian matrix [6, 7]. Despite the wide array of metrics currently in use, we are not aware of any work relating bounds on these metrics to bounds on higher order derivatives. We are not aware of any element metrics that quantify the magnitude of higher-order partial derivatives of the parametric mapping $\mathbf{x}_e : \hat{\Omega} \rightarrow \Omega_e$. Furthermore, we are not aware of any attempts to show that bounding any existing metrics implies bounds on higher-order derivatives.

To illustrate why this is a concern, consider the highly skewed element shown in Fig. 3, which has a scaled Jacobian of $J_S = 1$. While not all Jacobian based quality metrics will indicate that this element is of good quality, it is troubling that the most commonly used quality metric for curvilinear elements cannot distinguish between this highly skewed element and a purely linear triangle. Because of this, we argue that existing curvilinear element metrics are insufficient for guaranteeing that Cond. 2.3 holds, and as a result, are insufficient for guaranteeing that curvilinear elements will preserve optimal convergent rates under refinement.

Fig. 3 Highly distorted triangular Bernstein–Bézier element with a scaled Jacobian of $J_S = 1$.



3 Higher Order Quality Metrics for Bernstein–Bézier Elements

For simplicial Bernstein–Bézier elements, let $\{B_i^p(\boldsymbol{\xi})\}_{i \in I^p}$ denote the set of simplicial Bernstein basis polynomials of degree p defined over a reference domain $\hat{\Omega} \in \mathbb{R}^d$, where I^p is an index set over the degrees of freedom in the element. Now, let us define a set of control points $\{\mathbf{P}_i\}_{i \in I^p}$ in \mathbb{R}^d . Then, a simplicial Bézier element is simply defined through the mapping:

$$\mathbf{x}_e(\boldsymbol{\xi}) = \sum_{\mathbf{i} \in I^p} B_{\mathbf{i}}^p(\boldsymbol{\xi}) \mathbf{P}_{\mathbf{i}}$$

Theorem I For a simplicial Bernstein–Bézier element of degree p with control points $\{\mathbf{P}_{\mathbf{i}}\}_{\mathbf{i} \in I^p}$, the $\boldsymbol{\alpha}^{\text{th}}$ partial derivative of the mapping \mathbf{x}_e is bounded by:

$$\|D^{\boldsymbol{\alpha}} \mathbf{x}_e\|_{L^\infty(\hat{\Omega})} \leq \frac{p!}{(p - |\boldsymbol{\alpha}|)!} \max_{\mathbf{i} \in I^{p-|\boldsymbol{\alpha}|}} \left| \sum_{\mathbf{j} \in I^{\boldsymbol{\alpha}}} (-1)^{\boldsymbol{\alpha}+\mathbf{j}} \binom{\boldsymbol{\alpha}}{\mathbf{j}} \mathbf{P}_{\mathbf{i}+\mathbf{j}} \right|$$

Proof. We recognize that the derivatives of Bernstein polynomials are themselves Bernstein polynomials of a lower degree [8]. Recursively taking the derivative of the mapping \mathbf{x}_e yields the following equation for the $\boldsymbol{\alpha}^{\text{th}}$ partial derivative:

$$D^{\boldsymbol{\alpha}} \mathbf{x}_e = \frac{p!}{(p - |\boldsymbol{\alpha}|)!} \sum_{\mathbf{i} \in I^{p-|\boldsymbol{\alpha}|}} \left[B_{\mathbf{i}}^{p-|\boldsymbol{\alpha}|}(\boldsymbol{\xi}) \sum_{\mathbf{j} \in I^{\boldsymbol{\alpha}}} (-1)^{\boldsymbol{\alpha}+\mathbf{j}} \binom{\boldsymbol{\alpha}}{\mathbf{j}} \mathbf{P}_{\mathbf{i}+\mathbf{j}} \right]$$

Note, we take care to emphasize that the sum $\sum_{\mathbf{j} \in I^{\boldsymbol{\alpha}}}$ is a sum over a tensor product index set. This is a consequence of the fact that the partial derivative $\nabla^{\boldsymbol{\alpha}}$ has an inherently tensor product nature. Then, because the Bernstein polynomials satisfy positivity and partition of unity, the bounds of Theorem I are obtained. \square

For tensor product Bernstein–Bézier elements, let $\{B_{\mathbf{i}}^{\mathbf{p}}(\boldsymbol{\xi})\}_{\mathbf{i} \in I^{\mathbf{p}}}$ denote the set of tensor product Bernstein basis polynomials of degree \mathbf{p} defined over a reference domain $\hat{\Omega} \in \mathbb{R}^{d_r}$, where $I^{\mathbf{p}}$ is an index set over the degrees of freedom in the element. Now, let us define a set of control points $\{\mathbf{P}_{\mathbf{i}}\}_{\mathbf{i} \in I^{\mathbf{p}}}$ in \mathbb{R}^d . Then, a tensor product Bézier element is simply defined through the mapping:

$$\mathbf{x}_e(\boldsymbol{\xi}) = \sum_{\mathbf{i} \in I^{\mathbf{p}}} B_{\mathbf{i}}^{\mathbf{p}}(\boldsymbol{\xi}) \mathbf{P}_{\mathbf{i}}$$

Theorem II For a tensor product Bernstein–Bézier element of degree \mathbf{p} with control points $\{\mathbf{P}_{\mathbf{i}}\}_{\mathbf{i} \in I^{\mathbf{p}}}$, the $\boldsymbol{\alpha}^{\text{th}}$ partial derivative of the mapping \mathbf{x}_e is bounded by:

$$\|D^{\boldsymbol{\alpha}} \mathbf{x}_e\|_{L^\infty(\hat{\Omega})} \leq \frac{\mathbf{p}!}{(\mathbf{p} - \boldsymbol{\alpha})!} \max_{\mathbf{i} \in I^{\mathbf{p}-\boldsymbol{\alpha}}} \left| \sum_{\mathbf{j} \in I^{\boldsymbol{\alpha}}} (-1)^{\boldsymbol{\alpha}+\mathbf{j}} \binom{\boldsymbol{\alpha}}{\mathbf{j}} \mathbf{P}_{\mathbf{i}+\mathbf{j}} \right|$$

Proof. As before, we can write the derivatives of the Bernstein polynomials as Bernstein polynomials of lower degree:

$$D^{\boldsymbol{\alpha}} \mathbf{x}_e = \frac{\mathbf{p}!}{(\mathbf{p} - \boldsymbol{\alpha})!} \sum_{\mathbf{i} \in I^{\mathbf{p}-\boldsymbol{\alpha}}} \left[B_{\mathbf{i}}^{\mathbf{p}-\boldsymbol{\alpha}}(\boldsymbol{\xi}) \sum_{\mathbf{j} \in I^{\boldsymbol{\alpha}}} (-1)^{\boldsymbol{\alpha}+\mathbf{j}} \binom{\boldsymbol{\alpha}}{\mathbf{j}} \mathbf{P}_{\mathbf{i}+\mathbf{j}} \right]$$

and by positivity and partition of unity of the Bernstein polynomials, the desired bounds are obtained. \square

With the relevant theory established, we now demonstrate a particularly convenient property of the bounds presented in Theorem I and Theorem II. Consider the case of finding the higher order derivatives of a cubic Bernstein–Bézier triangle. Table 1 shows the bounding expressions for several derivatives of the mapping \mathbf{x}_e .

Table 1 Bounds on the derivatives of a cubic Bernstein–Bézier triangle.

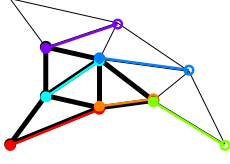
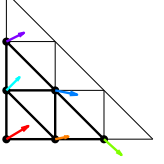
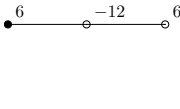
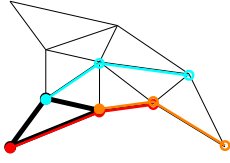
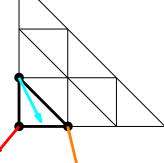
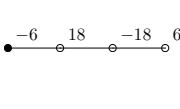
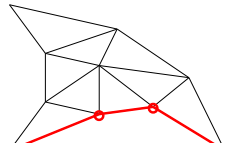
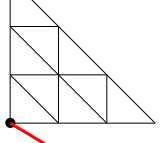
Derivative	Bound
$\frac{\partial \mathbf{x}_e}{\partial \xi_1}$	$\leq \max_{\mathbf{i} \in I^{p-1}} 3\mathbf{P}_{\mathbf{i}+\{1,0\}} - 3\mathbf{P}_{\mathbf{i}} $
$\frac{\partial^2 \mathbf{x}_e}{\partial \xi_1^2}$	$\leq \max_{\mathbf{i} \in I^{p-2}} 6\mathbf{P}_{\mathbf{i}+\{2,0\}} - 12\mathbf{P}_{\mathbf{i}+\{1,0\}} + 6\mathbf{P}_{\mathbf{i}+\{0,0\}} $
$\frac{\partial^3 \mathbf{x}_e}{\partial \xi_1^3}$	$= 6\mathbf{P}_{\{3,0\}} - 18\mathbf{P}_{\{2,0\}} + 18\mathbf{P}_{\{1,0\}} - 6\mathbf{P}_{\{0,0\}} $

From this, it is apparent that bounds on the derivatives of Bernstein–Bézier elements can be calculated using what is effectively a weighted finite difference method. To illustrate this notion, Table 2 shows finite difference stencils for the each of the derivatives shown in Table 1. While we have only shown a few explicitly calculated metrics here, the results of Theorem I and Theorem II can be used to calculate stencils for *any* simplicial or tensor product Bernstein–Bézier element.

4 Conclusions

We have presented a set of easily computable element quality metrics that are sufficient for guaranteeing that a mesh composed of curvilinear Bernstein–Bézier elements will preserve optimal convergence rates under refinement. While these metrics hold only for Bernstein–Bézier elements, they are extensible to other polynomial based elements through a simple change of basis. This note is a precursor to a larger text that will expand upon the basic ideas presented here [5]. Specifically, we extend the error bounds presented here to rational Bernstein–Bézier elements, and derive an analogous set of quality metrics for rational Bernstein–Bézier discretizations [3, 4]. We also present preliminary numerical results on how these metrics may be used for mesh optimization.

Table 2 Example of finding the Bézier coefficients for several different derivatives using a stencil.

Derivative	Stencil	Stencils Applied to the Physical Triangle	Bézier Coefficients of the Derivative
$\frac{\partial \mathbf{x}_e}{\partial \xi_1}$			
$\frac{\partial^2 \mathbf{x}_e}{\partial \xi_1^2}$			
$\frac{\partial^3 \mathbf{x}_e}{\partial \xi_1^3}$			

References

1. P. G. CIARLET AND P. A. RAVIART, *Interpolation theory over curved elements, with applications to finite element methods*, Computer Methods in Applied Mechanics and Engineering, 1 (1972), pp. 217–249.
2. S. DEY, R. M. O’BARA, AND M. S. SHEPHARD, *Curvilinear mesh generation in 3D*, in In Proceedings of the Eighth International Meshing Roundtable, John Wiley & Sons, 1999, pp. 407–417.
3. L. ENGVALL AND J. A. EVANS, *Isogeometric triangular Bernstein–Bézier discretizations: Automatic mesh generation and geometrically exact finite element analysis*, Computer Methods in Applied Mechanics and Engineering, 304 (2016), pp. 378–407.
4. ———, *Isogeometric unstructured tetrahedral and mixed-element Bernstein–Bézier discretizations*, Computer Methods in Applied Mechanics and Engineering, 319 (2017), pp. 83–123.
5. ———, *Mesh quality metrics for isogeometric bernstein-bézier discretizations*, Under Review, (2018).
6. A. GARGALLO-PEIRÓ, X. ROCA, J. PERAIRE, AND J. SARRATE, *Distortion and quality measures for validating and generating high-order tetrahedral meshes*, Engineering with Computers, 31 (2015), pp. 423–437.
7. R. POYA, R. SEVILLA, AND A. J. GIL, *A unified approach for a posteriori high-order curved mesh generation using solid mechanics*, Computational Mechanics, 58 (2016), pp. 457–490.
8. H. PRAUTZSCH, W. BOEHM, AND M. PALUSZNY, *Bézier and B-Spline Techniques*, Springer-Verlag New York, Inc., Secaucus, NJ, USA, 2002.